Kirkuk University Journal /Scientific Studies (KUJSS)
Volume 13, Issue 4, December 2018 , pp. (96-112)
ISSN: 1992-0849 (Print), 2616-6801 (Online)

Effect of Annealing on Some Properties of Zn_2SnO_4 Thin Films Prepared by PLD Technique

Sabri J. Mohammed[1], Kadhim A. Aadim[2], Maad M. Ameen[3]
[1]Department of Physics, College of Education, University of Tikrit, Tikrit, Iraq.
[2]Department of Physics, College of Sciences, University of Baghdad, Baghdad, Iraq.
[3]Department of Physics, College of Sciences, University of Kirkuk, Kirkuk, Iraq.
[1]sabri.jasim@tu.edu.iq, [2]Kadhim_adem@Scbaghdad.edu.iq, [3]Maad.mo.am@uokirkuk.edu.iq

Abstract

In this paper, the investigation of structural and optical properties of Zn_2SnO_4 thin films were studied. The films are performed on glass substrates by pulsed laser technique (PLD) using laser Nd: YAG at wavelength of 1064 nm with 800 mj laser energy using repetition rate of 6 Hz. and average 400 laser pulses at room temperature and annealing by tubular quartz furnace at temperature (573,773) K for 2 hours with air. XRD measurements showed that the structure for all samples is polycrystalline with a cubic nanostructure. Surface morphology was studied using scanning electron microscopy SEM and atomic force microscopy AFM. After annealing, the roughness of the surface and the mean grain size were increased. Optical properties as a function to wavelength in the range (300-1100 nm) have been studied. Absorption spectra of Zn_2SnO_4 thin films showed that absorption decreases with increasing annealing temperature. Direct energy gap for a Zn_2SnO_4 thin film was increases with increasing temperature for all samples due to crystal growth. The optical properties such as extinction coefficient, refractive index, and dielectric constant were also studied.

Keywords: annealing; Zn_2SnO_4 ; PLD technique.

DOI: http://doi.org/10.32894/kujss.2018.13.4.8

Kirkuk University Journal /Scientific Studies (KUJSS)
Volume 13, Issue 4, December 2018 , pp. (96-112)
ISSN: 1992-0849 (Print), 2616-6801 (Online)

تاثير التلدين على بعض خواص اغشية Zn_2SnO_4 الرقيقة المحضرة بتقنية PLD

صبري جاسم محمد[1]، كاظم عبد الواحد عادم[2]، معد محمد امين3

[1]قسم الفيزياء، كلية التربية للعلوم الصرفة، جامعة تكريت، تكريت، العراق.

[2]قسم الفيزياء، كلية العلوم، جامعة بغداد، بغداد، العراق.

[3]قسم الفيزياء، كلية العلوم، جامعة كركوك، كركوك، العراق.

[1]sabri.jasim@tu.edu.iq, [2]Kadhim_adem@Scbaghdad.edu.iq, [3]Maad.mo.am@uokirkuk.edu.iq

الملخص

تم في هذا البحث دراسة الخصائص التركيبية والبصرية لأغشية Zn_2SnO_4 الرقيقة والتي رسبت على قواعد زجاجية بواسطة تقنية ترسيب الليزر النبضي (PLD) باستخدام ليزر Nd: YAG النبضي عند طول موجة (1064 نانومتر) باستخدام طاقة ليزر (800 ملي جول). ومعدل تكرار قدره (6 Hz). باستخدام متوسط 400 نبضة ليزر. عند درجة حرارة الغرفة ثم التلدين بواسطة فرن الكوارتز الأنبوبي عند درجة حرارة (773، 573) كلفن لمدة ساعتين بوجود الهواء. أظهرت قياسات (XRDs) أن البنية البلورية لجميع العينات هي متعددة التبلور ذو تركيب مكعبي نانوي. تمت دراسة مورفولوجيا السطح باستخدام المجهر الإلكتروني الماسح (SEM) ومجهر القوة الذرية (AFM). بعد التلدين، تزداد خشونة السطح ومتوسط الحجم الحبيبي. تمت دراسة الخواص البصرية كدالة الى الطوال الموجي في المدى (300–1100 نانومتر). وأظهرت أطياف الامتصاص لأغشية Zn_2SnO_4 أن الامتصاصية تنخفض مع زيادة درجة حرارة التلدين. كما ان فجوة الطاقة المباشرة للأغشية تزداد مع زيادة درجة الحرارة لجميع العينات بسبب النمو البلوري. تمت دراسة الخصائص البصرية مثل معامل الخمود، معامل الانكسار ، وثابت العزل الكهربائي.

الكلمات الدالة: التلدين، Zn_2SnO_4، بتقنية PLD.

DOI: http://doi.org/10.32894/kujss.2018.13.4.8

Kirkuk University Journal /Scientific Studies (KUJSS)
Volume 13, Issue 4, December 2018 , pp. (96-112)
ISSN: 1992-0849 (Print), 2616-6801 (Online)

1. Introduction:

Zinc stannate Zn_2SnO_4, commonly known as zinc tin oxide ZTO, has been confirmed for high electron mobility (10-15 cm^2 / V.s). High electrical conductivity, Zn_2SnO_4 is a n-type transparent conductive oxide with a wide band gap of 3.7 eV [1]. It has wonderful visual optical properties that can be used in multiple fields such as solar cells, sensors to detect moisture and combustible gases. Fig 1. Crystalline structures of Zn_2SnO_4 (cubic spinel) [2]. Pulsed laser deposition is defined as a promising method for depositing metal thin films. The thickness of the films can be controlled by controlling the number of pulses [3]. The idea of PLD is simple. The laser pulse beam is concentrated on the outer surface of the target material. Where the laser is absorbed and leads to rapid evaporation of the target material [4]. Evaporated materials include highly ionized species. If the discharge is performed in a vacuum, it shows itself as a glowing plasma column directly opposite the target surface. In our current research, we study the structural and optical properties of Zn_2SnO_4 thin films grown on a glass slide produced by the PLD [5].

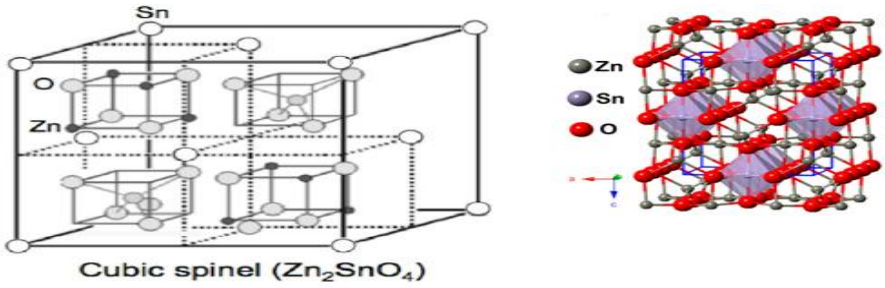

Fig. 1: Crystalline structures of zinc stannate Zn_2SnO_4 (cubic spinel) **[2].**

2. Theory:

Zinc oxide ZnO and tin oxide SnO_2 is the most promising candidate for the development of transparent conductive material. SnO_2 is an rutile tetragonal structure with oxygen deficient n- type degenerate semiconductor with wide band gap of 3.6 eV. Its high optical transparency and electrical conductivity leads to very appealing applications in spintronics device [6]. ZnO in view of its high transmission over a wide spectral range including the useful UV-vis region and other interesting characteristics such as low toxicity, relatively low cost, and stability in reductive chemical environments [7]. SnO_2 and ZnO thin films have attracted significant interest recently for use in optoelectronic application such as solar cells, flat panel displays, photonic devices, laser diodes and gas sensors. In the present study, Nanoparticle powders of zinc stannate in date spinel Zn_2SnO_4 were prepared by mixing stoichiometric amounts of tin

Kirkuk University Journal /Scientific Studies (KUJSS)
Volume 13, Issue 4, December 2018 , pp. (96-112)
ISSN: 1992-0849 (Print), 2616-6801 (Online)

oxide SnO_2 and zinc oxide ZnO, in the same molar ratio, ($ZnO:SnO_2$ = 1:1).The zinc stannate Zn_2SnO_4 films have the advantages of both ZnO and SnO_2,and are promising for solar cell and sensor applications [8].

3. Experimental Work:

Tin oxide Nanoparticles SnO_2 purity (99.98 %) powder by Sky Spring Nanoparticles, Inc. 2935 Westhollow Dr., Houston, Tx 77082. and zinc oxide ZnO Nano Powder, with purity (99.9%) by Nanjing Nano Technology. Prepared Zn_2SnO_4 by mixing stoichiometric amounts of tin oxide SnO_2 and zinc oxide ZnO, in the molar ratio, ($ZnO:SnO_2$ = 1:1) and ball milled for 1 hrs. to use it to make target as a disk of (1.5) cm diameter and (0.3) cm thickness using hydraulic piston type (SPECAC), under pressure of (6) tons for (15) minutes. finally the pellets were sintered in air at (1000 C˚) for (2) hrs.

PLD and deposition of thin film: We used glass slides (2.5 x 7.5 cm) that were cleaned with liquid soap. Then immersed in distilled water using an ultrasound device for 15 minutes to remove all dust and dirt. Dry it with a thin strip of cotton to be ready for deposition at room temperature. Use PLD technique using the laser Nd: YAG with (λ = 1064 nm) at power (800 mJ), under the vacuum (3×10^{-3} mp) using the double- stage rotary pump. Repeating frequency (6Hz) for laser pulse (400) is incident on the target surface with an angle of (45˚). A set of PLD system is given in Fig. 2. The distance between the target and the laser (10 cm) was determined ,and between the target and the glass slide (2 cm).

Annealing process: The annealing process was performed by a tubular quartz furnace Fig. 3. at a temperature of (573,773) K˚ for 2 hours with air.

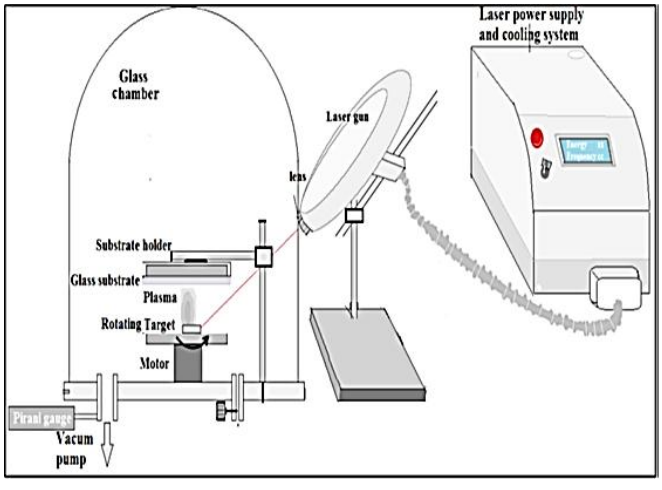

Fig. 2: Schematic of the PLD system [9]

Fig. 3: tubular quartz furnace.

Kirkuk University Journal /Scientific Studies (KUJSS)
Volume 13, Issue 4, December 2018 , pp. (96-112)
ISSN: 1992-0849 (Print), 2616-6801 (Online)

X-Ray Diffraction: The crystalline structure of the Zn_2SnO_4 thin films, which were deposited on glass slides by PLD method at RT, and (573,773 K˚) temperatures, was studied using x-ray diffraction techniques using (Bruker-D2 phaser vorsicht rontgenstrahl ung caution x-rays) device. This device registers the intensity as a function of the Bragg's angle [10]:

$$n\lambda = 2\, d_{hkl}\, sin\, \theta \quad (1)$$

Where Θ is the diffraction angle and λ is the XRD wavelength used. The grain size of the granularity *G.S* of the crystals, which is important in the study of X-ray spectrum characteristics, can be estimated by full width at half-maximum (FWHM) calculated by Scherrer equation [11]:

$$G.S = \frac{0.9\,\lambda}{FWHM\, Cos\theta} \quad (2)$$

Where θ is the Bragg's angle of the XRD Peak.

Measuring optical properties: The optical properties of thin films are affected by crystalline structure, thickness and type of materials used. The optical properties have been investigated using UV-visible spectral spectrometer (SP-8001) in the range (300-1100) nm. The output data from the absorption, wavelength, and transmitter are used in a computer program to measure all optical constants. The value of the energy gap (E_g) is graphically estimated by equation [12]

$$\alpha h\nu = B'\left(h\nu - {E_g}^{opt.}\right)^{\frac{1}{2}} \quad (3)$$

Were ${E_g}^{opt.}$ = is the optical energy gap ; h Blank's constant ; ν is the frequency of light; B' constant depends on the type of material.

When measuring absorption and transmittance spectra, we can know the behavior of the refractive index spectra *n* and extinction *k* of the ZTO [13].

$$k = \frac{\alpha\lambda}{4\pi} \quad (4)$$

$$n = \left(\frac{4R}{(R-1)^2} - k^2\right)^{1/2} - \frac{(R+1)}{(R-1)} \quad (5)$$

where R is the reflectance. The real and imaginary part of dielectric constant can be calculated by using the following equations [14]:

$$\varepsilon_r = n^2 - k^2 \quad (6)$$

Kirkuk University Journal /Scientific Studies (KUJSS)
Volume 13, Issue 4, December 2018 , pp. (96-112)
ISSN: 1992-0849 (Print), 2616-6801 (Online)

$$\varepsilon_i = 2nk \quad (7)$$

4. Results and Calculations:

4.1 Structure measurement: Fig. 4 shows the X-ray diffraction for Zn_2SnO_4 thin films. We can observe that the deposited film has polycrystalline structure, XRD diffraction results at room temperature have two peak located at 2θ values (29.0499, 34.2162) corresponding to (220) and (311) direction respect to Zn_2SnO_4 crystals. and with annealing at (573,773) K˚, It shows several Six diffraction peaks at 2θ values of (29.0499º, 34.2162º, 36.1758º, 41.5558º, 54.9881º and 60.3325º).

These were assigned to the diffraction lines produced by (220), (311), (222), (400), (511) and (440) of the (cubic spinel) structure of Zn_2SnO_4 confirmed by standard data. We can see many other peaks are detected in the XRD pattern for the hexagonal ZnO at 2θ values of (31.6152º, 47.6128º, 56.5558º and 62.791º) and tetragonal SnO_2 at 2θ values of (26.5202º, 33.7886º, 37.8504º and 51.7102º).

The FWHM decrease with increasing annealing temperature indicate on increasing particle size. The intensity of the peaks increases as the temperature of the annealing increases, which means that the crystallization of the film improves as the temperature of the annealing increases.

The annealing process reduces crystalline defects and reduce optical dispersion. Table 1 shows the experiment and the standard peaks from (JCPDS Joint Committee on Powder Diffraction Standards - (ICDD) International Centre for Diffraction Data) cards number (24-1470, 96-210-4744 and 96-901-1663) Returns to Zn_2SnO_4, SnO_2 and ZnO Respectively.

Kirkuk University Journal /Scientific Studies (KUJSS)
Volume 13, Issue 4, December 2018 , pp. (96-112)
ISSN: 1992-0849 (Print), 2616-6801 (Online)

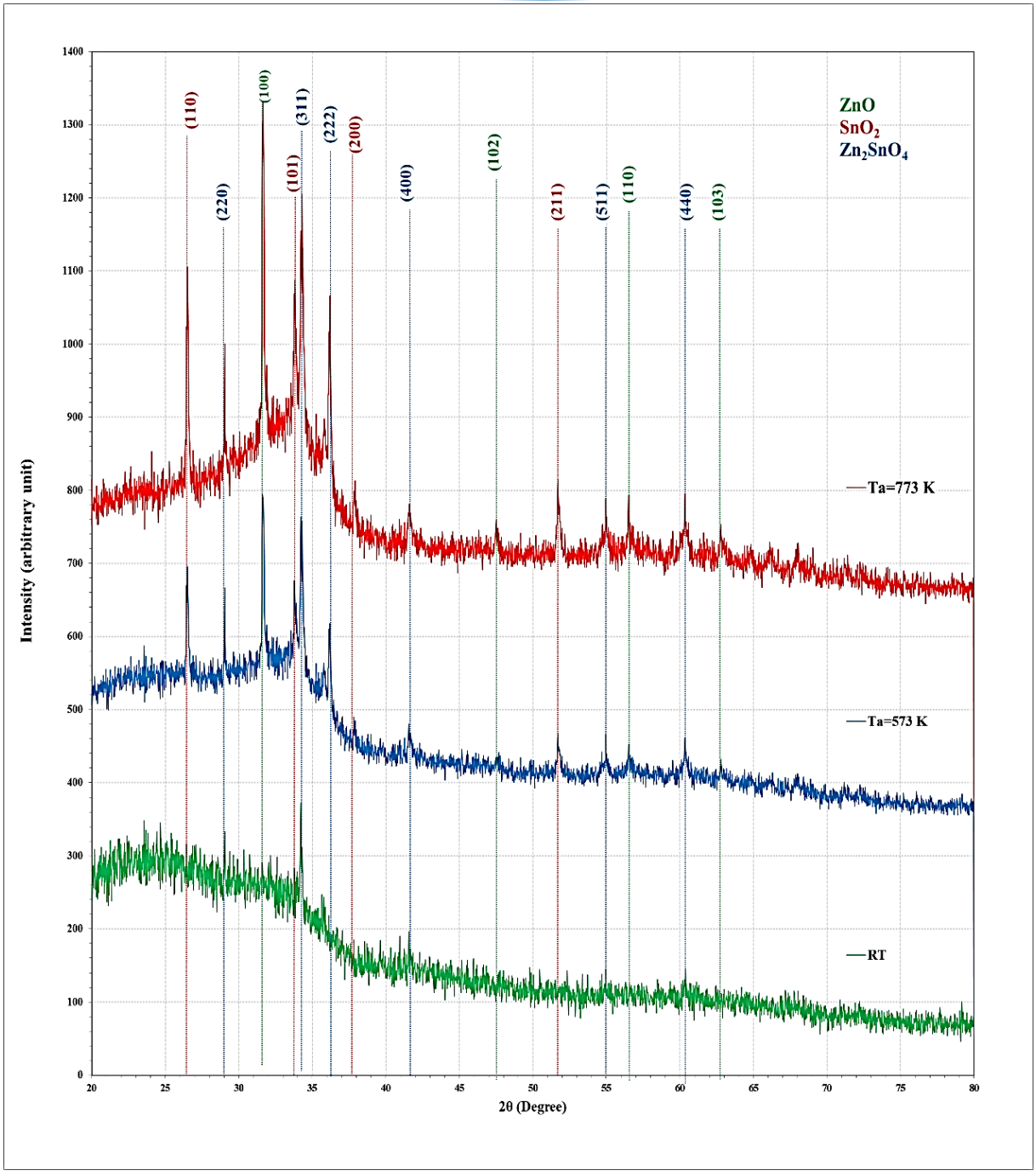

Fig. 4: X-ray diffraction patterns of Zn_2SnO_4 films deposited at RT and different annealing temperatures (573,773) K˚.

Kirkuk University Journal /Scientific Studies (KUJSS)
Volume 13, Issue 4, December 2018 , pp. (96-112)
ISSN: 1992-0849 (Print), 2616-6801 (Online)

Table 1: Structural parameters: Inter-planar spacing, crystalline size of Zn_2SnO_4 films deposited at RT and annealing at (573,773) K˚.

T_a (K)	2θ (Deg.)	FWHM (Deg.)	d_{hkl} Exp.(Å)	G.S (nm)	Hkl	d_{hkl} Std.(Å)	Phase	Card No.
RT	29.0499	0.2494	3.0714	32.9	(220)	3.0621	Zn_2SnO_4	24-1470
	34.2162	0.3207	2.6185	25.9	(311)	2.6130	Zn_2SnO_4	24-1470
573	26.5202	0.2138	3.3583	38.2	(110)	3.3498	SnO_2	96-210-4744
	29.0499	0.2138	3.0714	38.4	(220)	3.0621	Zn_2SnO_4	24-1470
	31.6152	0.1781	2.8277	46.4	(100)	2.8137	Hex. ZnO	96-901-1663
	33.7886	0.2137	2.6507	38.9	(101)	2.6439	SnO_2	96-210-4744
	34.2162	0.2850	2.6185	29.2	(311)	2.6130	Zn_2SnO_4	24-1470
	36.1758	0.2494	2.4810	33.5	(222)	2.4991	Zn_2SnO_4	24-1470
	37.8504	0.2494	2.3750	33.7	(200)	2.3686	SnO_2	96-210-4744
	41.5558	0.3563	2.1714	23.9	(400)	2.1651	Zn_2SnO_4	24-1470
	47.6128	0.3563	1.9083	24.4	(102)	1.9110	Hex. ZnO	96-901-1665
	51.7102	0.3563	1.7664	24.8	(211)	1.7642	SnO_2	96-210-4744
	54.9881	0.4988	1.6686	18.0	(511)	1.6647	Zn_2SnO_4	24-1470
	56.5558	0.6057	1.6260	14.9	(110)	1.6245	Hex. ZnO	96-901-1663
	60.3325	0.4988	1.5329	18.4	(440)	1.5304	Zn_2SnO_4	24-1470
	62.7910	0.6057	1.4787	15.4	(103)	1.4772	Hex. ZnO	96-901-1663
773	26.5202	0.2100	3.3583	38.9	(110)	3.3498	SnO_2	96-210-4744
	29.0499	0.1581	3.0714	51.9	(220)	3.0621	Zn_2SnO_4	24-1470
	31.6508	0.1425	2.8246	58.0	(100)	2.8137	Hex. ZnO	96-901-1663
	33.8242	0.2010	2.6480	41.3	(101)	2.6439	SnO_2	96-210-4744
	34.2874	0.2494	2.6132	33.4	(311)	2.6130	Zn_2SnO_4	24-1470
	36.1758	0.2138	2.4810	39.1	(222)	2.4991	Zn_2SnO_4	24-1470
	37.9216	0.2494	2.3707	33.7	(200)	2.3686	SnO_2	96-210-4744
	41.5914	0.3206	2.1696	26.5	(400)	2.1651	Zn_2SnO_4	24-1470
	47.5059	0.2851	1.9124	30.5	(102)	1.9110	Hex. ZnO	96-901-1665
	51.6746	0.2851	1.7675	31.0	(211)	1.7642	SnO_2	96-210-4744
	54.9525	0.3919	1.6696	22.9	(511)	1.6749	Zn_2SnO_4	24-1470
	56.5558	0.2425	1.6260	37.2	(110)	1.6245	Hex. ZnO	96-901-1663
	60.3682	0.2138	1.5321	43.0	(440)	1.5304	Zn_2SnO_4	24-1470
	62.7910	0.2851	1.4787	32.7	(103)	1.4772	Hex. ZnO	96-901-1663

4.2 Morphology Analysis :

4.2.1. Atomic Force Microscope (AFM): Fig.5 shows the AFM images and their granularity accumulation distribution for Zn_2SnO_4 thin films deposited on glass slides by PLD at (RT) and annealing at (573,773 K˚). This Figure and Table 2 illustrate that the Average Diameter, roughness Average and RMS are increased with increased annealing temperature. This may

Kirkuk University Journal /Scientific Studies (KUJSS)
Volume 13, Issue 4, December 2018 , pp. (96-112)
ISSN: 1992-0849 (Print), 2616-6801 (Online)

be due to the bigger clusters formed by the coalescence of two or more grains and decrease or disappearance the grain bounders. This result is identical with [15].

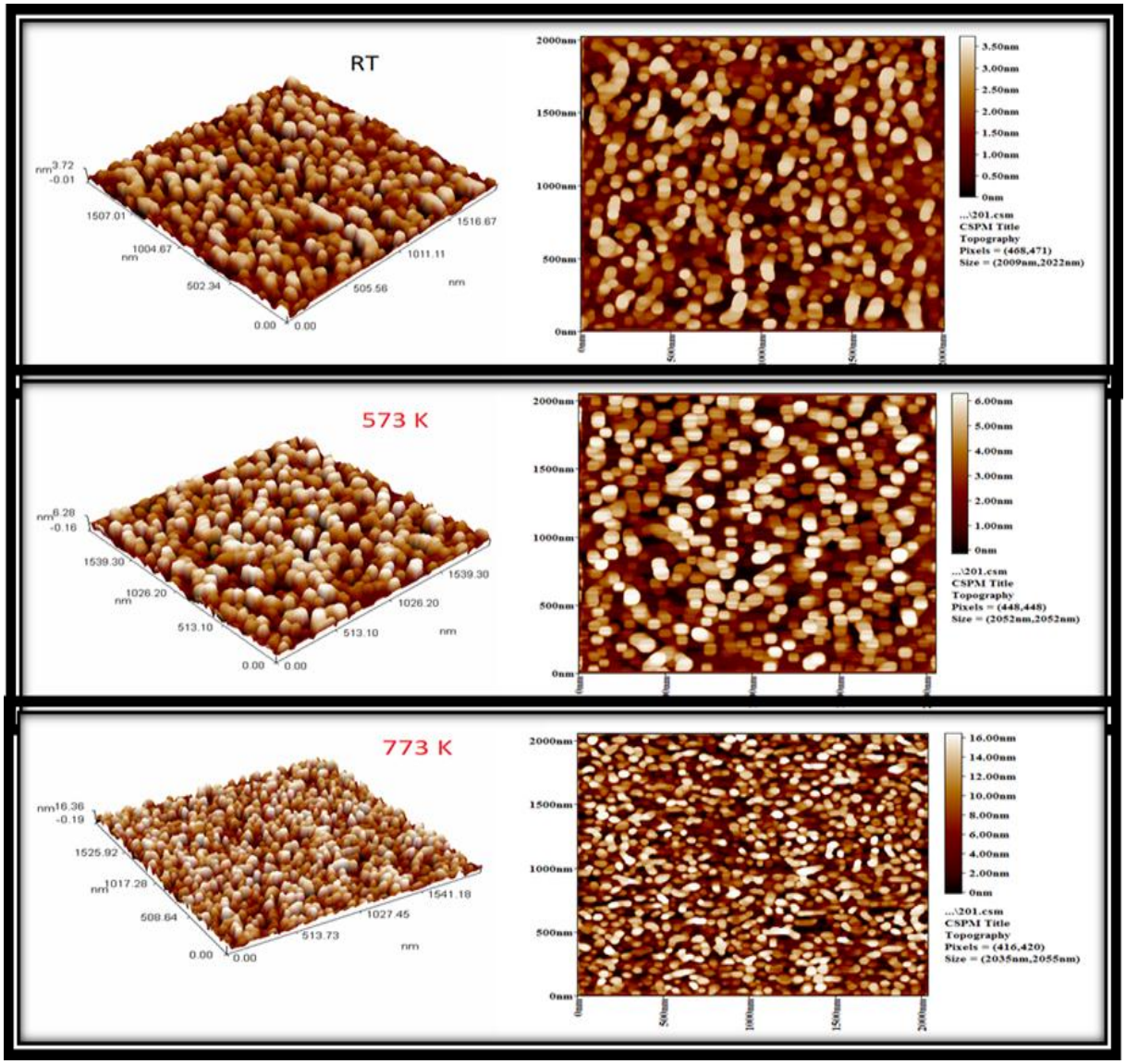

Fig. 5: AFM images and their granulate accumulation for Zn_2SnO_4 thin films deposited at RTand annealing at (573,773) K˚.

Table 2: AFM parameters (Average Diameter, roughness Average and RMS) for Zn_2SnO_4 films deposited at RT and annealing at (573,773) K˚.

Temperature (K˚)	Average Diameter (nm)	roughness Average (nm)	Root Mean Square (nm)
RT	63.96	0.832	3.17
573	69.65	1.61	6.44
773	80.31	4.14	16.5

Kirkuk University Journal /Scientific Studies (KUJSS)
Volume 13, Issue 4, December 2018 , pp. (96-112)
ISSN: 1992-0849 (Print), 2616-6801 (Online)

4.2.2. scanning electron microscopy (SEM): Fig. 6a,7a shows the SEM images of Zn_2SnO_4 films deposited on the glass substrates by the PLD at RT and its temperature 773 K˚. Fig. 6b,7b shows the SEM analysis images with the IMAGEJ program. The surface of all thin films is known as a cluster of granules known as clusters, which represents homogeneous surface morphology of thin films. The Zn_2SnO_4 thin film has a perfectly uniform surface with no holes. With a wide distribution of particles of about 20-50 nm, which agrees with the XRD result. With annealing, the average size of aggregated particles increases obviously. This result may be attributed to higher atom mobility with the increase in temperature which causes more effective recrystallization and grain growth of the films that result in larger grains. This result was in agreement with [16].

4-2.3 EDAX Study: The EDAX pattern shown in Fig. (6-c), (7-c) confirms the presence of Zn and Sn. The observed Zn/Sn ratio for the films measured from the EDX measurement of the Zn_2SnO_4 stoichiometry for both the sediment by PLD in RT and annealed at (773) K˚.

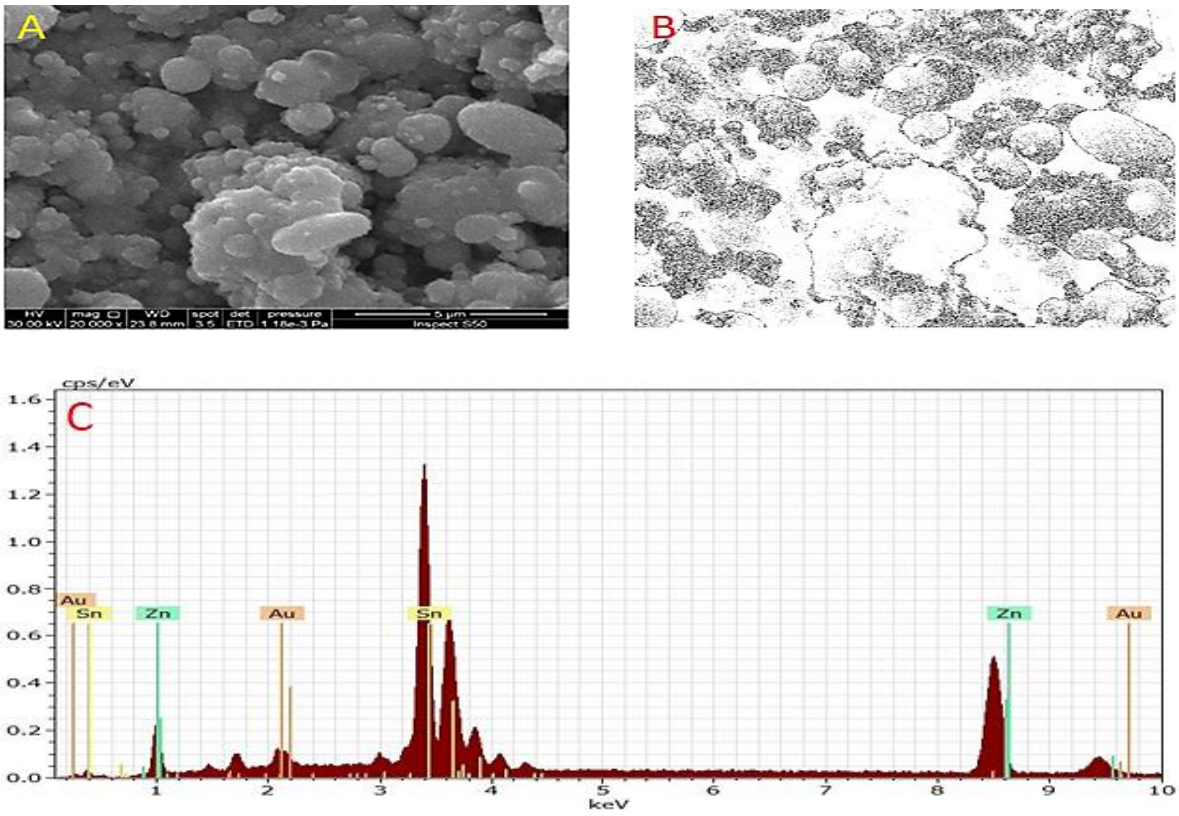

Fig. 6:. Zn_2SnO_4 thin films deposited at RT (a) SEM image, (b) Analyze SEM image by IMAGEJ program, (C) Typical EDAX pattern.

Kirkuk University Journal /Scientific Studies (KUJSS)
Volume 13, Issue 4, December 2018 , pp. (96-112)
ISSN: 1992-0849 (Print), 2616-6801 (Online)

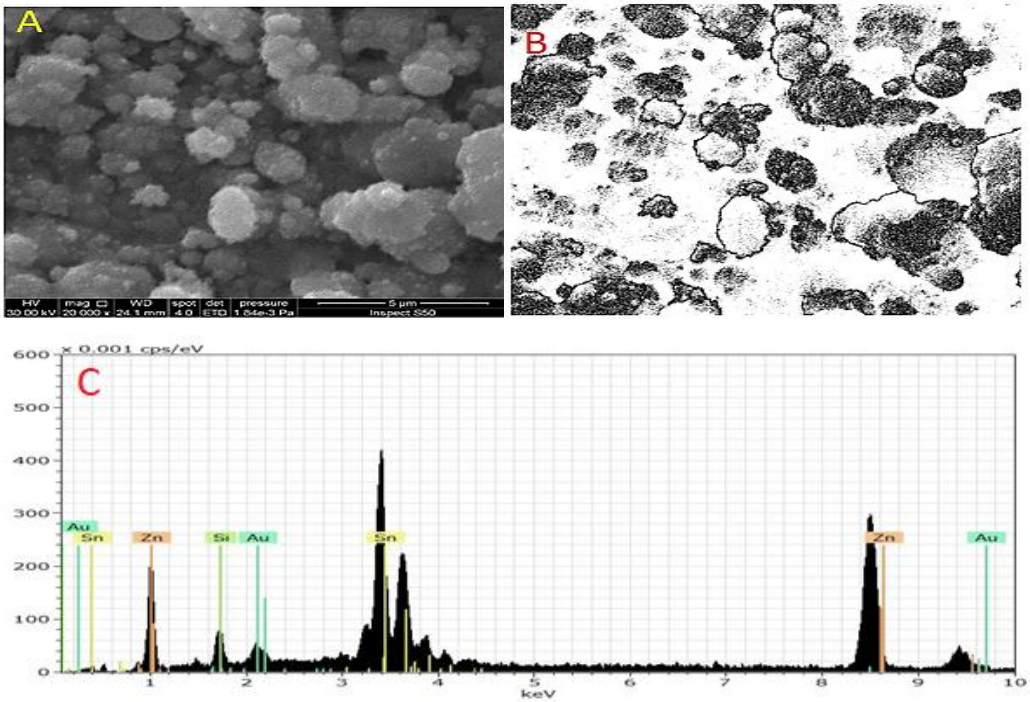

Fig. 7: Zn_2SnO_4 thin film annealed at (773) K˚ temperature (a) SEM image, (b) Analyze SEM image by IMAGEJ program, (C) Typical EDAX pattern.

4.3 Optical measurement :

4.3.1 Absorbance spectrum: Fig. 8 shows the absorption spectrum as a function of the wavelength for a range (300-1100) nm. It can be seen that when the temperature of the annealing increases, as a result of increase the crystallization, the amount of absorption decreases. The reason is the decay and disappearance of donor levels (i.e localized states) within forbidden energy gap and conduction band. This leads to an increase in the value of E_g. In the near UV-visible light region, a strong photo-absorption at a wavelength of 330 nm is presented. This result is in agreement with [2].

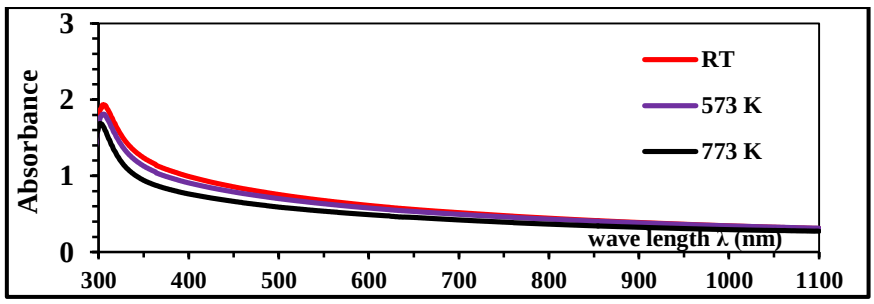

Fig. 8: shows absorbance for Zn_2SnO_4 films deposited at RT and annealing at (573,773) K˚.

Kirkuk University Journal /Scientific Studies (KUJSS)
Volume 13, Issue 4, December 2018 , pp. (96-112)
ISSN: 1992-0849 (Print), 2616-6801 (Online)

4.3.2 Absorption Coefficient (α): Fig. 9 show the optical absorption coefficient α as a function of wavelength (λ) for Zn_2SnO_4 thin films. we can see from this Figure that the values of α becomes higher ($\alpha > 10^4$) cm^{-1}, this supports to expect a direct electronic transition occurs in these regions. also we found that the α of the Zn_2SnO_4 films has a strong absorption coefficient at the short wavelength region (high energies). On the other hand, it is found that the value of α decreases with increasing of annealing temperature due to increase energy gap E_g. The α values are approximately equal to the reported values by [2].

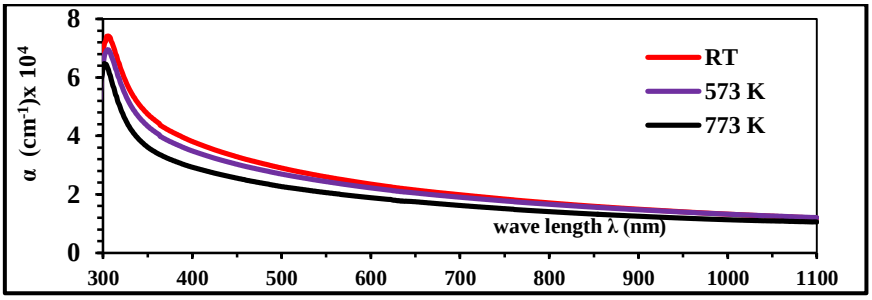

Fig. 9: shows Absorption Coefficient for Zn_2SnO_4 films deposited at RT and annealing at (573,773) k

4-3-3 The Optical Energy Gap (E_g): The values of the optical energy gap E_g for nanoparticles Zn_2SnO_4 thin films are determined using eq (3). A plot of relation $(\alpha h\nu)^2$ versus photon energy (hν) and the choice of the desired linear section. From Fig. 10, we can see that the energy gap was increased from (3.55-3.7) eV, as a result of the increasing of the annealing temperature, This is due to the growth of grain size and the reduction of the number of grain boundaries. Increase E_g as a result of reducing the amount of absorption, this may lead to improved the crystal structures, which leads to the reduction of defects (tail state) in the forbidden gap and this leads to an increase in the E_g. The values of the approximate absorption coefficient with the values reported by [17].

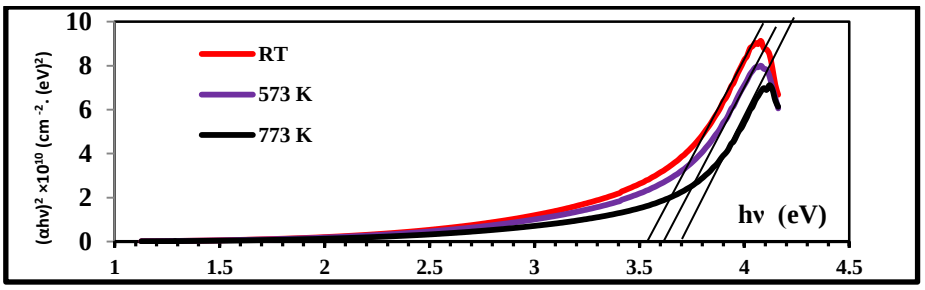

Fig. 10: $(\alpha h\nu)^2$ as function of energy photon for nanostructure Zn_2SnO_4 thin films deposited at RT and annealing at (573,773) K˚.

Kirkuk University Journal /Scientific Studies (KUJSS)
Volume 13, Issue 4, December 2018 , pp. (96-112)
ISSN: 1992-0849 (Print), 2616-6801 (Online)

4.3.4 Optical Constants:

4.3.4.a Extinction Coefficient (*K*): According to the formula. (4) The behavior of the extinction coefficient (*K*) is similar to the behavior of the absorption coefficient (α). Fig. 11 shows the extinction coefficient (*K*) as a function of the wavelength (λ) of Zn_2SnO_4 films at RT and (573,773) K˚. We can see from Fig. 11 and Table. 3 that the extinction coefficient (*K*) decreases generally with increased temperatures. This result is consistent with [18].

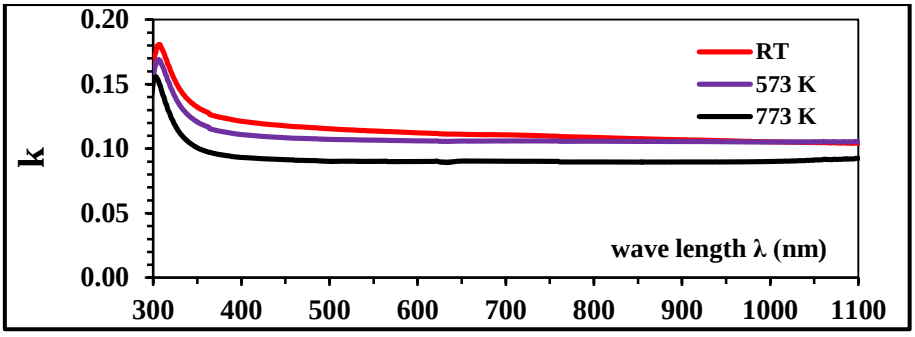

Fig. 11: Extinction coefficient *K* with wavelength for nanostructure Zn_2SnO_4 thin films deposited at RT and annealing at (573,773) K˚.

4.3.4.b Refractive Index (*n*) :From Fig. 12 we see that the value of Refractive index (*n*) for all films is approximately limited by (2.2.5). we can show from these figures that (*n*) increases slightly with increasing of annealing temperature and the reason for this, first the growth of grain size which causes increases of Surface roughness which means increases of the reflection where the refractive index depends on it. Secondly, reduced porosity and increased density of the thin films material due to annealing which in turn decreases the light velocity thereby causing a change in the refractive index This is consistent with [19].

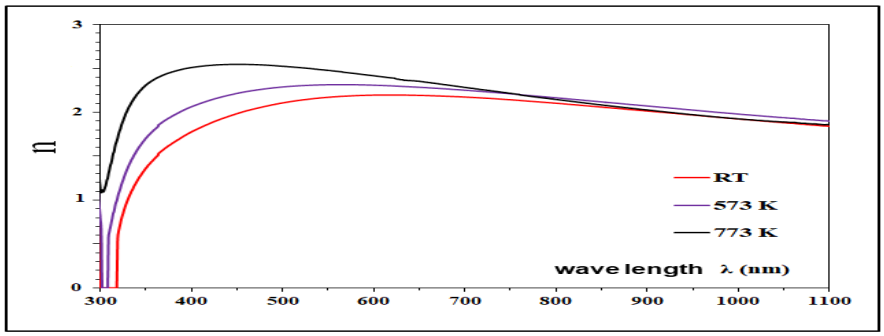

Fig. 12: The Variation of The Refractive Index *n* With Wavelength for Zn_2SnO_4 thin films deposited at RT and annealing at (573,773) K˚.

Kirkuk University Journal /Scientific Studies (KUJSS)
Volume 13, Issue 4, December 2018 , pp. (96-112)
ISSN: 1992-0849 (Print), 2616-6801 (Online)

4.3.5 Dielectric Constant: The electrical dielectric Constant was studied in real and imaginary parts as a function of wavelength. Fig. 13 (a) shows the relationship between the real portion of the dielectric constant versus the wavelength where we see that all samples behave like refractive index (n) samples due to the small value of (k^2) compared to (n^2) based on eq. (6) Fig. 13 (b) shows the relationship between the imaginary portion of the dielectric constant versus the wavelength. We found that all samples behaves like extinction coefficients (k) based on equation (7). This means that the real part increases with increasing of annealing temperature The value of the imaginary part decreases as the temperature rises. It can be observed that the values of the real portion of the dielectric constant decrease with increasing wave lengths and actual values of the real part are greater than the values of the imaginary part as shown in Table 3 . These measurements correspond with [18].

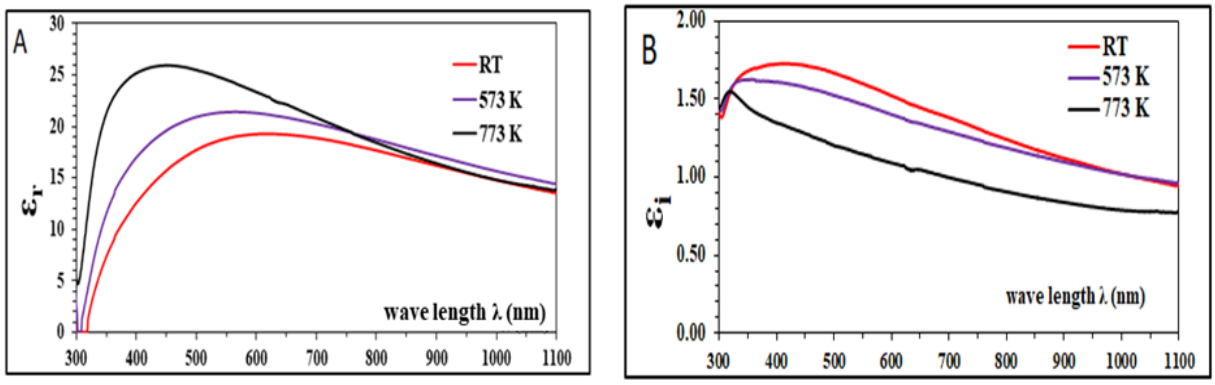

Fig. 13: The Variation of The Dielectric Constants (a)-real part (ε_r) and (b)- imaginary (ε_i) parts With Wavelength of Zn_2SnO_4 Films at RT and annealing at (573,773) K˚.

Table 3: Values of Absorption Coefficient **α** ,Refractive index (n), Extinction coefficient (k), Real (ε_r) and Imaginary (ε_i) Dielectric Constant for Zn_2SnO_4 films (at 500 nm wavelength) and The Optical Energy Gap (E_g).

Ta (K˚)	***α (cm^{-1})***	***K***	***n***	***ε_r***	***ε_i***	***E_g* eV**
RT	28983	0.12	2.1	17.689	1.7167	3.55
573	26920	0.11	2.25	20.932	1.6355	3.6
773	22653	0.09	2.5	25.472	1.3659	3.7

5. Conclusion:

Structural and optical properties analysis show that pulsed laser deposition technique is a useful method for the deposition of Zn_2SnO_4 thin films on glass substrates. Post-annealing process helps to improve the crystalline quality thin films. All the films show polycrystalline with cubic nanostructure. XRD, AFM and SEM indicate that the Average Diameter, roughness Average and RMS of the nanoparticles thin film increases with increasing the annealing temperature. direct energy band gap values increases with increasing annealing temperatures about 3.7 eV for the film annealed at 773 K for 2 hour.

References:

[1] Z. Li, Y. Zhou, C. Bao, G. Xue, J. Zhang, J. Liu, T. Yuab and Z. Zou, "***Vertically building Zn_2SnO_4 nanowire arrays on stainless steel mesh toward fabrication of large-area, flexible dye-sensitized solar cells***", The Royal Society of Chemistry, Nanoscale, 4, 3490 (2012).

[2] S. Baruah and J. Dutta, "***Zinc stannate nanostructures:hydrothermal synthesis***", science and technology of advanced materials, 12, 013004 (2011).

[3] C. Viespe , I. Nicolae, C. Sima, C. Grigoriu, and R. Medianu,"***ITO thin films deposited by advanced pulsed laser deposition***", Thin Solid Films 515, 8771 (2007).

[4] R. Vinodkumar, K.J.Lethy, D.Beena, A.P.Detty, I.Navasa, U. V. Nayar, V. P. Mahadevan Pillai,V. Ganesan, and V. R. Reddy." ***Effect of ITO buffer layers on the structural, optical and electrical properties of ZnO multilayer thin films prepared by pulsed laser deposition technique***", Solar Energy Materials & Solar Cells, 94, 68 (2010).

[5] M. A. H. Fenollosa, M. C. Lopez,V. Donderis, M. Gonzalez, B. Marí and J. R. Ramos-Barrado, "***Role of precursors on morphology and optical properties of ZnS thin films prepared by chemical spray pyrolysis*** ", Journal of Thin Solid Films, 516, 1622 (2008).

[6] S. K. Sinha,T. Rakshit, S. K. Ray, I. Manna, "***Characterization of ZnO–SnO2 thin film composites prepared by pulsed laser deposition***", Applied Surface Science 257,10551 (2011).

[7] P. Wang, J. Zhao, J. Liu, L. Wei, Z. Liu, L. Guan, G. Cao,"***Stabilization of organometal halide perovskite films by SnO2 coating with inactive surface hydroxyl groups on ZnO nanorods***" Journal of Power Sources, 339, 51, (2017).

[8] T. Tharsika, A. S. M. A. Haseeb, M. F. M. Sabri, "***Structural and optical properties of ZnO–SnO2 mixed thin films deposited by spray pyrolysis***" Thin Solid Films 558, 283 (2014).

[9] Kadhem A. Aadim, Abdulmajeed E. Ibrahim, and Qutaibah A. Abduljabbar, "***Optical and Electrical Properties of $(SnO_2)X(In_2O_3)_{1-X}$ thin Films Prepared by Pulse Laser Deposition Technique***", International Journal of Physics, 5(4), 116 (2017).

[10] Charles Kittel, "***Introduction to Solid State Physics***", 7th Ed., john wiley and son, Inc., new york (1996).

[11] E. L. Foletto, M. A. Mazutti, A. Cancelier, E. Marlon de Moraes Flores, E. I. Muller, L. S. F. Pereira, O. Chiavone-Filho and A. Gündel, "***Effect of Microwave Power on the Zn_2SnO_4 Synthesis and Its Use for Photodegradation of Phenol***", Journal of Chemistry and Chemical Engineering, 8, 794 (2014).

[12] M. M. Jaculine, C. J. Raj, and S. J. Das, "***Hydrothermal synthesis of highly crystalline Zn_2SnO_4 nanoflowers and their optical properties***", Journal of Alloys and Compounds, 577, 131 (2013).

[13] V.V. Starikov, M. M. Ivashchenko, A. S. Opanasyuk, V. L. Perevertaylo, "***Surfase morphology and optical properties of CdSe films obtained by the closespaced vacuum sublimation technique***", Journal of Nano - and Electronic Physics, 1(4), 119 (2009).

[14] M. M. Abdel-Aziz , I. S. Yahia , L. A. Wahab , M. Fadel ,and M. A. Afifi " ***Determination and analysis of dispersive optical constant of TiO_2 and Ti_2O_3 thin films***", Applied Surface Science, 252, 8163 (2006).

[15] T. J. Coutts, D. L. Young, X. Li, W. P. Mulligan, and X. Wu, "***Search for improved transparent conducting oxides: A fundamental investigation of CdO,Cd_2SnO_4,and Zn_2SnO_4***", Journal of Vacuum Science & Technology, 18(6), 2646 (2000).

[16] Y. Li, A. Pang, X. Zheng, M. Wei. "***CdS quantum-dot-sensitized Zn_2SnO_4 solar cell***" Electrochimica Acta, 56, 4902 (2011).

[17] B. S. P. de Raadt, " ***growth and characterization of zinc tin oxide thin films deposited by co-injection spatial atomic layer deposition***", MSc. thesis, Eindhoven University of Technology, (2015).

[18] A. O. Salohub, A. A. Voznyi, O. V. Klymov, N.V. Safryuk, D.I. Kurbatov, and A.S. Opanasyuk,"***Determination of fundamental optical constants of Zn_2SnO_4 films***" , Semiconductor Physics, Quantum Electronics & Optoelectronics, 20(1), 79 (2017).

[19] K. Satoh, Y. Kakehi, A. Okamoto, S. Murakami, F. Uratani and T. Yotsuya " ***Influence of Oxygen Flow Ratio on Properties of Zn_2SnO_4 Thin Films Deposited by RF Magnetron Sputtering***", Japanese Journal of Applied Physics, 44(1), 34 (2005).